Density functional theory analysis of dopants in cupric oxide

Yuan Peng, Zhen Zhang, Thien Viet Pham, Yang Zhao, Ping Wu et al.

Citation: J. Appl. Phys. **111**, 103708 (2012); doi: 10.1063/1.4719059
View online: http://dx.doi.org/10.1063/1.4719059
View Table of Contents: http://jap.aip.org/resource/1/JAPIAU/v111/i10
Published by the American Institute of Physics.

Density functional theory analysis of dopants in cupric oxide

Yuan Peng,[1] Zhen Zhang,[2,a)] Thien Viet Pham,[1] Yang Zhao,[1] Ping Wu,[3] and Junling Wang[1,a)]
[1]*School of Materials Science and Engineering, Nanyang Technological University, 50 Nanyang Avenue, Singapore 639798*
[2]*Institute of High Performance Computing, 1 Fusionopolis Way, #16-16 Connexis, Singapore 138632*
[3]*Engineering Product Development, Singapore University of Technology and Design, 20 Dover Drive, Singapore 138682*

(Received 12 February 2012; accepted 10 April 2012; published online 21 May 2012)

Fabrication of both p-type and n-type cupric oxide is of great importance for the large-scale photovoltaic application. Our first-principles density functional theory calculations confirm that copper vacancy can lead to good p-type conduction in CuO, while oxygen vacancy is a deep donor. To investigate electrical conduction in CuO, we calculated the defect formation energies as well as their ionization levels for several potential acceptors and donors. Our results indicate that Li and Na are shallow acceptors and their formation energies are low in oxygen rich environment. However, it is also found that n-type conduction is relatively hard to induce by donors, as most donors have deep transition levels in the band gap and/or high formation energies. Hf and Zr have the shallowest ionization levels of around 0.2 eV below the conduction band minimum, but their formation energies are relatively high, limiting the electrical conductivity of doped CuO. Our study explains why it is hard to obtain n-type conduction in CuO. © *2012 American Institute of Physics*. [http://dx.doi.org/10.1063/1.4719059]

I. INTRODUCTION

Monoclinic cupric oxide (CuO) is a semiconductor with an experimental band gap of about 1.3 eV.[1–6] It is a very promising material for the large-scale photovoltaic application because of its suitable band gap (ideal for sunlight absorption), abundance, and low extraction cost.[7] A CuO *p-n* homojunction solar cell has a theoretical maximum conversion efficiency of 31%,[8,9] better than that of a single crystal Si solar cell. Experimentally, undoped pure CuO is usually p-type due to the intrinsic copper vacancies, and the reported electrical conductivity is only about 0.01-0.001 S/cm.[3–6] Even though a few groups have reported n-type conduction in sputtered and thermally oxidized copper oxides recently,[10–12] the underlying mechanism is still under debate. Therefore, to reach the full potential of CuO, it is of great importance to identify suitable dopants in CuO for both p-type and n-type conduction. A theoretical study on this topic may offer some directions for experimental investigations.

The electronic structure of CuO has been calculated using density functional theory (DFT) with local spin density approximation (LSDA), which however fails to predict the semiconducting ground state.[13–15] Although some advanced methods such as the self-interaction correction (SIC) and the GW approximation provide nearly perfect descriptions of the excited state properties of CuO,[16,17] they demand heavy computing power, and are still not for large systems, such as the supercells needed for defect/dopant calculations. An alternative is the LSDA+U method, which takes into account the on-site repulsion among localized *d-d* electrons by adding the Hubbard term. It has proven to be very successful in describing transition metal oxides, including CuO.[18,19] Wu *et al.* have used LSDA+U method to study the native point defects in CuO.[20] They concluded that V_{Cu} (copper vacancy) is a shallow acceptor, but V_o (oxygen vacancy), Cu_i (copper interstitial), and Cu_O (copper antisite) are all deep donors, which suggest that CuO is intrinsically a p-type semiconductor, and n-type conduction in undoped CuO is unlikely.

Relevant theoretical studies on the extrinsic doping in CuO are still missing in the literature, which however could provide important and effective guidance for further experimental investigations. In this study, we perform DFT calculations using the LSDA+U method to evaluate the cation substitutions that may improve the p-type and n-type conduction of CuO. We have made the initial selection of dopants based on two criteria. First, the element should have a higher/lower valence state compared to that of Cu for donors/acceptors, respectively. Second, its ionic radii should be comparable with that of Cu^{2+} (0.72 Å) to make sure that negligible strain energy is introduced to the CuO host. With these constrains, group IA elements Li^{1+} (0.60 Å), Na^{1+} (0.95 Å) are considered as p-type acceptors, and group IIIA elements Al^{3+} (0.50 Å), Ga^{3+} (0.62 Å) and In^{3+} (0.81 Å), group IVB elements Ti^{4+} (0.68 Å), Zr^{4+} (0.80 Å) and Hf^{4+} (0.79 Å) are selected as potential n-type dopants (donors).

II. COMPUTATIONAL DETAILS

The calculations were performed using DFT as implemented in the VASP code within the projector augmented wave (PAW) method.[21,22] The pseudopotential approach was adopted, where Cu $3d^{10}\,4s^1$ and O $2s^2\,2p^4$ orbitals were treated in the basis. For the calculation of dopants, Li $1s^2\,2s^1$, Na $2p^6\,3s^1$, Al $3s^2\,3p^1$, Ga $4s^2\,3d^{10}\,4p^1$, In $5s^2\,4d^{10}\,5p^1$,

a)Authors to whom correspondence should be addressed: Electronic addresses: zhangz@ihpc.a-star.edu.sg and jlwang@ntu.edu.sg.

Ti $3p^6\ 4s^2\ 3d^2$, Zr $4s^2\ 4p^6\ 5s^2\ 4d^2$, and Hf $5p^6\ 6s^2\ 5d^2$ were considered as valence electrons. All calculations were performed with an energy cutoff of 600 eV, which has been tested for convergence before any structural optimization. To describe the correlation effect in CuO, the semi-empirical LSDA+U method was used, where the strong Coulomb repulsion between localized Cu 3*d* electrons was treated by adding a Hubbard-U term to the effective potential.[18] To calculate the lattice parameters and band structure of CuO unit cell, a Monkhost-Pack grid of $8 \times 8 \times 8\,k$ points was used to integrate the first Brillouin zone, and an antiferromagnetic spin ordering was assumed for CuO.[25] The ground state lattice parameters and atomic positions of pure CuO are obtained by conducting full relaxation calculations under 20 fixed volumes, and fitting the equation-of-state (EOS) functions. Then, a $2 \times 3 \times 2$ supercell with a $3 \times 3 \times 3$ grid of *k* points was used for the calculations on doped systems, where one copper atom is replaced by an extrinsic dopant. All the ions were fully relaxed while keeping the lattice parameters fixed to those of undoped CuO until the Hellman-Feynman forces were less than 10 meV/Å. The total energy was converged to be within 1 meV for all systems.

The theoretical band gap depends on the value of Hubbard-U as shown in Fig. 1(a). In this study, a Hubbard energy of $U_{eff} = 7.5$ eV ($U = 7.5$ eV and $J = 0$ eV) was adopted following Dudarev's approach.[23] The theoretical band gap was calculated to be 1.32 eV and is close to the experimental value (1.2–1.5 eV) and previous theoretical study.[16–18,20] Our calculated lattice parameters for the unit cell are $a = 4.56$ Å, $b = 3.27$ Å, $c = 4.96$ Å, $\beta = 100.2$, and $u = -0.593$ (Table I), which are in a good agreement with experimental values.[24] In Fig. 1(b), we show the total density of states (DOS) of CuO unit cell and partial DOS for Cu and O, respectively, where both the valence and conduction bands are composed of hybridized Cu 3*d* and O 2*p* states.

The formation energy of the dopant at the Cu site in CuO can be expressed by

$$\Delta E^q = (E^q_{\text{defect}} - E_{\text{perfect}}) + (\mu_{\text{Cu}} - \mu_{\text{D}}) + qE_{\text{F}}, \qquad (1)$$

where E^q_{defect} is the total energy of the supercell with a dopant in the charged state *q*, E_{perfect} is the total energy of the perfect supercell, and μ_{D} and μ_{Cu} denote the corresponding atomic chemical potentials. E_{F} is the Fermi energy of CuO. A monopole correction, $\frac{e^2q^2\alpha}{L\varepsilon}$, is applied to the total energy of the charged systems, where α is the Madelung constant, *L* is the size of the supercell, and ε is the dielectric constant of CuO ($\varepsilon = 18$ from Ref. 26). The transition level equals to the Fermi energy for which the charged states *q* and q' have the same formation energy. From Eq. (1), one obtains

$$\varepsilon(q/q') = \frac{E^q_{\text{defect}} - E^{q'}_{\text{defect}}}{q' - q}. \qquad (2)$$

Under thermal equilibrium conditions, the steady production of host material, CuO, should satisfy the following equation:

$$\mu_{\text{Cu}} + \mu_{\text{O}} = \Delta H_f^{\text{CuO}} = -2.04 \text{ eV},$$

where μ_{D} and μ_{O} are chemical potentials of Cu and O source, respectively, and ΔH_f^{CuO} is the formation enthalpy for CuO per formula. The upper bound of μ_{O} (O rich) is limited by O_2 gas formation

$$\mu_{\text{O}} = 0 \text{ eV} \text{ and } \mu_{\text{Cu}} = -2.04 \text{ eV}.$$

The lower limit of μ_{O} (O poor) is set by Cu_2O formation

$$2\mu_{\text{Cu}} + \mu_{\text{O}} \le \Delta H_f^{\text{Cu}_2\text{O}} = -2.14 \text{ eV},$$

yielding:

$$\mu_{\text{O}} = -1.94 \text{ eV} \text{ and } \mu_{\text{Cu}} = -0.1 \text{ eV}.$$

For doping study, the chemical potentials of dopants also need to satisfy other constraints to avoid the formation of dopant-related phases. For example, for Al doping, the chemical potential of Al is constrained by $\mu_{\text{Al}} < 0$ and $2\mu_{\text{Al}} + 3\mu_{\text{O}} \le \Delta H_f^{\text{Al}_2\text{O}_3} = -17.47$ eV. The formation enthalpies of the dopant oxides are also calculated and listed in Table II. Note that the differences between experimental and theoretical values are all very small, demonstrating the accuracy of our calculations. Also listed in Table II are the differences of chemical potentials for copper and all dopants, which are lower under oxygen-poor condition than under oxygen-rich condition for the donors, and vice versa for the acceptors.

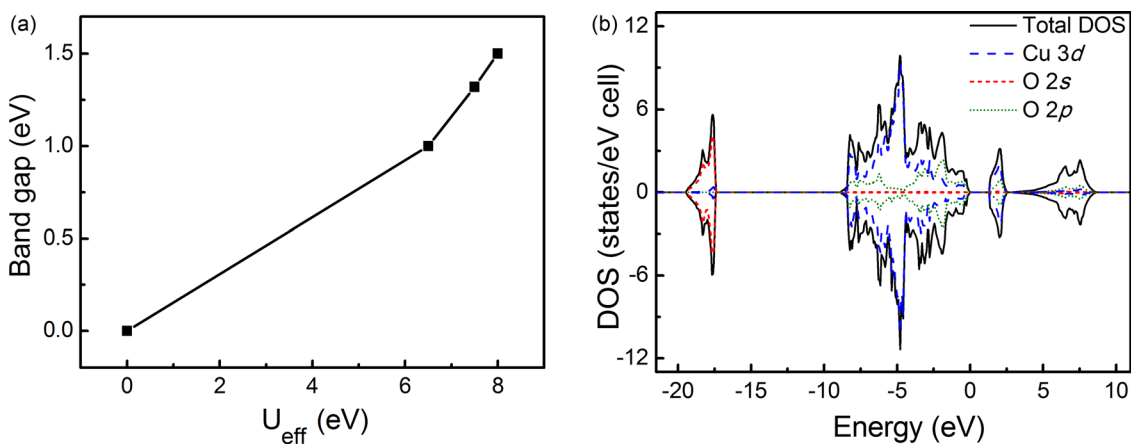

FIG. 1. (a) Dependence of band gap on the value of U_{eff} with the LSDA + U method and (b) the total and partial DOS of CuO unit cell for $U_{eff} = 7.5$ eV.

TABLE I. Calculated lattice parameters, band gaps, E_g and spin moments m of CuO using LSDA and LSDA + U ($U_{eff} = 7.5$ eV). Experimental data were taken from Refs. 1, 2, and 24.

	LSDA	LSDA + U	Experiment	Ref. 20
a (Å)	4.05	4.57	4.65	4.55
b (Å)	4.06	3.27	3.41	3.34
c (Å)	5.06	4.96	5.11	4.99
β	90.02	100.2	99.48	99.5
u	0.50	0.59	0.58	0.58
E_g (eV)	0.00	1.32	1.2–1.5	1.00
m (μ_B)	0.00	0.63	0.65	0.60

III. RESULTS AND DISCUSSION

A. Intrinsic defects in pure CuO

The formation energies of intrinsic copper and oxygen vacancies under both O-rich and O-poor conditions are shown in Fig. 2 as functions of Fermi level. The Fermi level is varied between the valence band maxima (VBM) ($E_F = 0$ eV) and conduction band minima (CBM) ($E_F = 1.32$ eV). For intrinsic copper vacancy, V_{Cu}, we observe a V_{Cu}^{1-}/V_{Cu}^{2-} transition at about 0.2 eV above the VBM, which could correspond to the experimentally observed p-type activation energy of 0.1 eV.[4] Meanwhile, V_{Cu}^{2-} is the dominant defect and has very low formation energy under O-rich condition, which therefore explains the p-type conductivity in CuO. It is also clear that the formation energy and thus concentration of copper vacancy can be affected by oxygen partial pressure in the experiment. Under O-poor condition, the formation energy of V_{Cu} surpasses that of oxygen vacancy V_O for p-type CuO. However, the V_O^0/V_O^{1+} and V_O^{1+}/V_O^{2+} transition levels are both deep in the band gap. So, the electron carriers emitted by oxygen vacancy are not enough to convert the conductivity from p-type to n-type.

B. Group IA acceptor dopants

The formation energies of group IA acceptors under the O-rich and O-poor conditions are shown in Fig. 3 as functions of Fermi level. Without the formations of Li_2O and Na_2O, the derived upper-limit chemical potentials for Li and Na are –2.23 and –1.22 eV under O-poor condition and −3.20 and −2.18 eV under O-rich condition.

In Fig. 3, the line for a specific charged acceptor state is only plotted within the range where it has the lowest formation energy among all the charged states. Hence, the change in slope corresponds to the transitions between the charged dopant states. The formation energies of −1 charged Li_{Cu} and Na_{Cu} defects are negative throughout the range of Fermi level under the O-rich condition, indicating that Li and Na can spontaneously substitute the Cu site. The p-type conductivity of a semiconductor depends on the transition energy levels of acceptors with respect to the VBM. For Li and Na, the (0/−1) transition levels are very shallow, only 0.03 and 0.09 eV above the VBM, respectively. Moreover, the formation energies of these acceptors are lower than that of any intrinsic vacancies. Therefore, the p-type conduction could be further enhanced by the extrinsic doping with Li and Na. Experimentally it was indeed found that Li-doped CuO single crystal shows improved p-type conduction.[4]

C. Group IIIA donor dopants

The calculated formation energies as functions of Fermi level for group IIIA donors (Al, Ga, and In) under O-poor and O-rich conditions are shown in Fig. 4, respectively. Without the formation of Al_2O_3, Ga_2O_3, In_2O_3, and elemental metals, the derived upper-limit chemical potentials for Al, Ga, and In are −5.83, −2.74, and −2.03 eV under O-poor condition and −8.74, −5.65, and −4.94 eV under O-rich condition. From Fig. 4, it is clear that the formation energies of Al, Ga, and In dopants are much lower under the O poor condition than that under the O rich condition. Also, under O rich, the formation energy of copper vacancy is lower than those of the dopants. Thus, under the O poor condition, group IIIA dopants could reach the highest solubility in CuO. The formation energy of Ga_{Cu} is smaller than that of Al_{Cu} and In_{Cu}.

For group IIIA donors, there are two possible charge states, 0 and +1 as shown in Fig. 4. The +1 charge state (contributes one electron to the material) is stable at low

TABLE II. Ionic radius (Å) and Pauling electronegativity of tested dopants. The valence states of corresponding ions of dopants are assumed to be +3 for group IIIA elements and +4 for group IVB and −1 for group IA elements. Calculated enthalpies of formation (ΔH_f) for dopant oxides as well as chemical potential differences between copper and dopants ($\mu_{Cu} - \mu_D$) are also presented.

	Al	Ga	In	Ti	Zr	Hf	Li	Na
Ionic radius (Å)	0.50	0.62	0.81	0.68	0.80	0.79	0.60	0.95
Electronegativity	1.61	1.81	1.78	1.54	1.33	1.30	0.98	0.93
				ΔH_f (eV)				
	α-Al_2O_3 (R-3c)	β-Ga_2O_3 (C2/m)	In_2O_3 (Ia-3)	TiO_2 (P42/mnm)	ZrO_2 (P21/c)	HfO_2 (P21/c)	Li_2O (Fm-3 m)	Na_2O (Im-3 m)
Experiment[27]	−17.40	−11.30	−9.60	−9.80	−11.40	−11.60	−6.4	−4.37
This work	−17.47	−11.29	−9.87	−10.32	−11.37	−12.08	−6.2	−4.30
				$\mu_{Cu} - \mu_D$ (eV)				
	Al	Ga	In	Ti	Zr	Hf	Li	Na
O-rich	6.70	3.60	2.90	8.28	9.33	10.04	1.16	0.14
O-poor	5.72	2.64	1.93	6.34	7.39	8.10	2.13	1.12

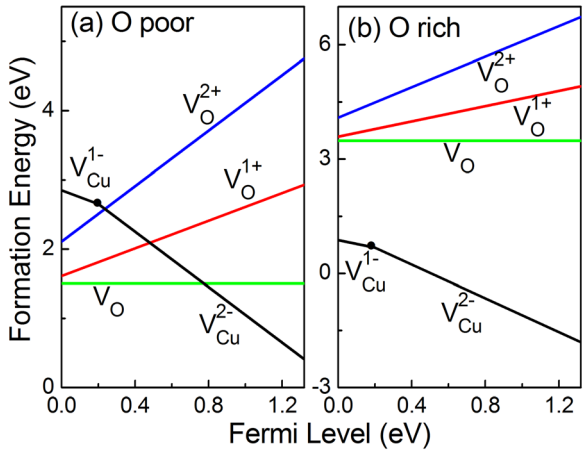

FIG. 2. Formation energies of intrinsic vacancies as functions of the Fermi level under (a) oxygen-poor condition, and (b) oxygen-rich condition. While all the states of oxygen vacancy are shown, only the lowest formation energy states of copper vacancy are shown.

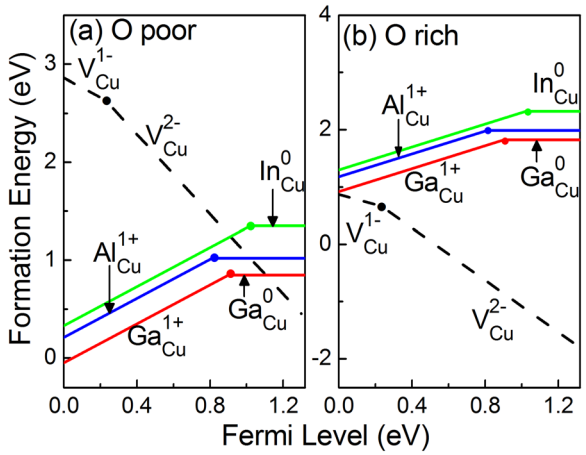

FIG. 4. Calculated formation energies for group IIIA donors (Al, Ga, and In) as functions of the Fermi level under (a) oxygen poor condition, and (b) oxygen rich condition. Only the lowest formation energy states are shown. The calculated formation energy of oxygen vacancy and copper vacancy is also shown in the figure for comparisons.

Fermi energies and becomes unstable at high Fermi energies. The position of donor ionization level with respect to the CBM is essential for n-type conduction. Note that the (0/+1) transition level for Al_{Cu} locates at 0.51 eV below the CBM, and neutral Al_{Cu}^{0} is the dominant defect state in the doped CuO. At room temperature, the probability to excite the valence electron of Al in CuO to the conduction band is almost zero. This result agrees with the experimental finding that n-type conduction was not observed in Al-doped CuO.[4] Also, Ga_{Cu} can hardly contribute electrons to the conduction band due to the fact that its transition energy of 0.42 eV below CBM is also very deep. However, relatively shallower donor levels locating at 0.30 eV below the CBM are observed for In. But its relatively higher formation energy effectively constrains the number of electrons.

D. Group IVB donor dopants

Our calculated formation energies as functions of Fermi level for the group IVB elements under O-poor and O-rich conditions are shown in Fig. 5. Without the formation of TiO_2, ZrO_2, HfO_2, and their elemental metals, the derived upper-limit chemical potentials for Ti, Hf, and Zr are −6.44, −7.49, and −8.2 eV at O-poor condition and −10.32, −11.37, and −12.08 eV at O-rich condition, respectively. For group IVB dopants, their maximum solubility in CuO also happens under O-poor condition. The formation energy of Ti_{Cu} is lower than that of Zr_{Cu} and Hf_{Cu}. The doping with group IVB donors leads to three possible charge states (0, +1, and +2) in the CuO band gap. It is possible for these dopants to contribute two valence electrons to the conduction band. Relatively shallow donor levels for Zr and Hf, corresponding to the (0/+1) transition, are found at 0.20 eV and 0.19 eV below the CBM, respectively, which makes it possible to obtain n-type CuO through Zr and Hf doping. However, similar to the case for group IIIA donors, their formation energies are high, which could greatly reduce the concentration of carriers.

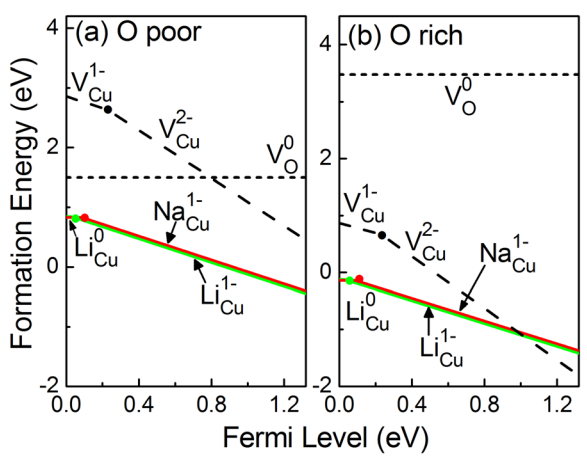

FIG. 3. Calculated formation energies for group IA acceptors, Li and Na, as functions of the Fermi level under: (a) oxygen-poor condition and (b) oxygen-rich condition. Only the lowest formation energy states are shown. The calculated formation energy of oxygen vacancy and copper vacancy is also shown in the figure for comparisons.

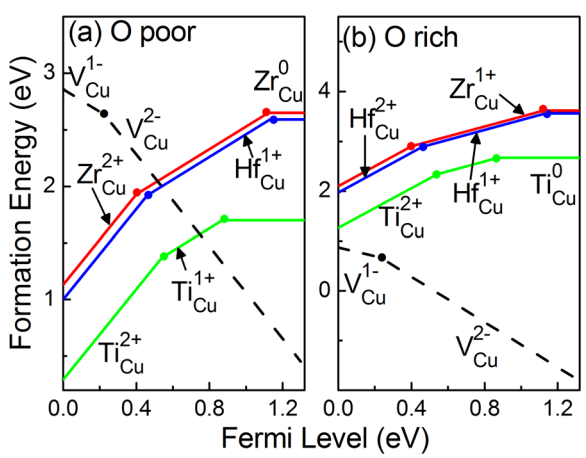

FIG. 5. Calculated formation energies for group IVB donors (Ti, Zr, and Hf) as functions of the Fermi level under (a) oxygen poor condition and (b) oxygen rich condition. Only the lowest formation energy states are shown. The calculated formation energy of oxygen vacancy and copper vacancy is also shown in the figure for comparisons.

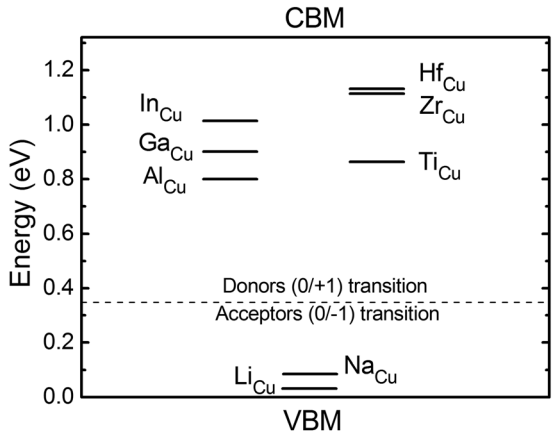

FIG. 6. Ionization levels in the band gap for the dopants in CuO. VBM denotes valence band maximum and CBM represents conduction band minimum.

E. Transition levels

The calculated donor levels for all the possible dopants are summarized and listed in Fig. 6. For group IIIA and IVB dopants, it is found that the ionization levels generally decrease as atomic number increases within the same group. This systematic variation could be explained by the electronegativity of the doping element. The Pauling electronegativity of Ti is 1.54, higher than 1.33 for Zr and 1.3 for Hf. Therefore, Ti atom attracts electrons more strongly and requires higher energy to be ionized than Zr and Hf. The same behaviour is found for group IIIA Al, Ga, and In.

IV. CONCLUSIONS

In summary, we have conducted a systematic investigation of potential p-type and n-type dopants (through cation substitution) for CuO using first-principles DFT calculations. We found that the ionization levels of Ti_{Cu}, Al_{Cu}, Ga_{Cu}, and In_{Cu} are too deep to contribute to the n-type conduction in CuO. Furthermore, two possible n-type dopants with relatively shallow ionization levels have been identified, which are Zr and Hf. But their formation energies are high which could make the doping process challenging. On the other hand, p-type conduction could be easily enhanced by Li and Na doping, which features lower dopant formation energies, as well as shallow ionization levels ($\sim$0.03 eV) in the CuO band gap. It is also observed that the ionization levels is closely related to the electronegativity of dopants, while less electronegative element tends to give rise to a shallower donor level. We hope that this theoretical investigation could shed light on the confusions about the conductivity type of the CuO and offer directions for further experimental study.

ACKNOWLEDGMENTS

This work is supported by the Singapore National Research Foundation under Project No. NRF-CRP5-2009-04. Additional computing resources are provided by Institute of High Performance Computing, Singapore.

[1]F. Marabelli, G. B. Parravicini, and F. Salghetti-Drioli, Phys. Rev. B **52**, 1433 (1995).
[2]J. Ghijsen, L. H. Tjeng, J. V. Elp, H. Eskes, J. Westerink, and G. A. Sawatzky, Phys. Rev. B **38**, 11322 (1988).
[3]Y. K. Jeong and G. M. Choi, J. Phys. Chem. Solids **57**, 81 (1996).
[4]S. Suda, S. Fujitsu, K. Koumoto, and H. Yanagida, Jpn. J. Appl. Phys., Part 1 **31**, 2488 (1992).
[5]M. Muhibbullah, M. O. Hakim, and M. G. M. Choudhury, Thin Solid Films **423**, 103 (2003).
[6]K. Nakaoka, J. Ueyama, and K. Ogura, J. Electrochem. Soc. **151**, C661 (2004).
[7]C. Wadia, A. P. Alivisatos, and D. Kammen, Environ. Sci. Technol. **43**(6), 2072 (2009).
[8]W. Shockley and H. J. Queisser, J. Appl. Phys. **32**(3), 510 (1961).
[9]M. C. Hanna and A. J. Nozik, J. Appl. Phys. **100**(7), 074510 (2006).
[10]H. C. Lu, C. L. Chu, C. Y. Lai, and Y. H. Wang, Thin Solid Films **517**, 4408 (2009).
[11]C. L. Chu, H. C. Lu, C. Y. Lo, C. Y. Lai, and Y. H. Wang, Physica B **404**, 4831 (2009).
[12]V. Figueiredo, E. Elangovan, G. Goncalves, P. Barquinha, L. Pereira, N. Franco, E. Alves, R. Martins, and E. Fortunato, Appl. Surf. Sci. **254**, 3949 (2008).
[13]K. Terakura, T. Oguchi, A. R. Williams, and J. Kubler, Phys. Rev. B **30**, 4373 (1984).
[14]M. Grioni, M. T. Czyzyk, F. M. F. de Groot, J. C. Fuggle, and B. E. Watts, Phys. Rev. B **39**, 4886 (1989).
[15]W. Y. Ching, Y. N. Xu, and K. W. Wong, Phys. Rev. B **40**, 7684 (1989).
[16]A. Svane and O. Gunnarsson, Phys. Rev. Lett. **65**, 1148 (1990).
[17]M. Takahashi and J.-I. Igarashi, Phys. Rev. B **56**, 12818 (1997).
[18]V. I. Anisimov, J. Zaanen, and O. K. Andersen, Phys. Rev. B **44**, 943 (1991).
[19]R. C. Albers, N. E. Christensen, and A. Svane, J. Phys.: Condens. Matter **21**, 343201 (2009).
[20]D. Wu, Q. Zhang, and M. Tao, Phys. Rev. B **73**, 235206 (2006).
[21]G. Kresse and J. Furthmuller, Phys. Rev. B **54**, 11169 (1996).
[22]P. E. Blochl, Phys. Rev. B **50**, 17953 (1994).
[23]S. L. Dudarev, G. A. Botton, S. Y. Savrasov, C. J. Humphreys, and A. P. Sutton, Phys. Rev. B **57**, 1505 (1998).
[24]S. Asbrink and L. J. Norrby, Acta Crystallogr. **B26**, 8 (1970).
[25]B. X. Yang, T. R. Thurston, J. M. Tranquada, and G. Shirane, Phys. Rev. B **39**, 4343 (1989).
[26]T. Kimura, Y. Sekio, H. Nakamura, T. Siegrist, and A. P. Ramirez, Nature Mater. **7**, 291 (2008)
[27]O. Kubaschewski, *Materials thermochemistry* (Pergamon Press in Oxford, New York, 1993).